Part I

Introduction to Micro-Pulling-Down Method

1 Micro-Pulling-Down (μ-PD) and Related Growth Methods

Valery I. Chani

Abstract. A comparison of the μ-PD technique with other (sometimes very similar) melt growth configurations is made. Both well known and relatively rare procedures are reviewed. An attempt is made to classify melt growth methods where crystal growth is achieved through displacement of the solidified material in the downward direction. This classification scheme was based on the appearance and spatial positioning of the basic components of the growth system: the melt, the solids, the crucible, etc. The advantages and shortcomings of μ-PD are summarized from the point of view of the process, the degree of control over the shape of the crystal, and the ability of the technique to be industrialized. Some historical comments demonstrate the evolution of the method from methodological and technical points of view.

There are a number of melt growth techniques that permit the production of relatively uniform quasi-one-dimensional single-crystalline materials. Most of them were well classified and described in [1–3] in terms of the arrangement of the growth system: the relative positions of the feed material, the crucible, the melt, and the crystalline solid produced. Micro floating zone methods and techniques that involve pulling from the die have been concluded to be the two main principles suitable for the growth of small-diameter fiber crystals from the melt. Laser-heated pedestal growth (LHPG), the micro-pulling-down (μ-PD) technique, edge-defined film-fed growth (EFG, also known as the Stepanov method), as well as the inverted Stepanov method have been considered to be the systems most suited to the production of fiber-shaped materials (crystals with diameters of about 1 mm and aspect ratios of 10^2 or greater).

The term "micro-pulling-down" that appears on the cover of this book does not provide an exceptionally clear explanation of the actual performance of this system. However, it does describe the organization and general behavior of the growth unit well. "Pulling-down" represents the direction of solidification. On the other hand, "micro" reflects the presence of microchannel(s) or micro-outlets (sometimes called nozzles) about 1 mm in diameter at the bottom of the melt reservoir (the crucible). These channels allow mass (melt) transport between the liquid mass in the crucible, the meniscus zone below the crucible bottom, and the growth interface.

The performance of such a crucible depends on the presence of an additional dense (liquid or solid) substance just below the bottom (Fig. 1.1).

In general, the crucible behaves like conventional crucible (i.e., one without holes) when there is no such a substance: the melt remains stationary inside the crucible due to surface tension (Fig. 1.1, left). This behavior also depends on the wetting properties of the melt. However, the crucible becomes "bottomless" when the dense substance (seed or crystal) contacts the crucible (initiating crystal growth); from this moment onwards the melt can flow through the opening(s) due to the action of surface forces and gravity.

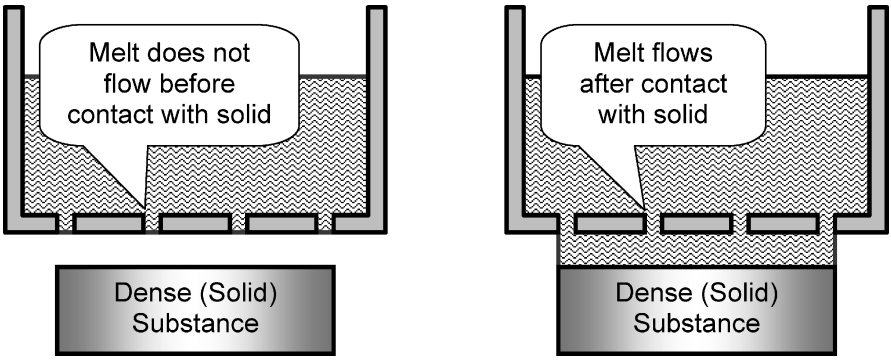

Fig. 1.1. Behavior of the melt in the crucible container with micro-channels (outlets) on the bottom

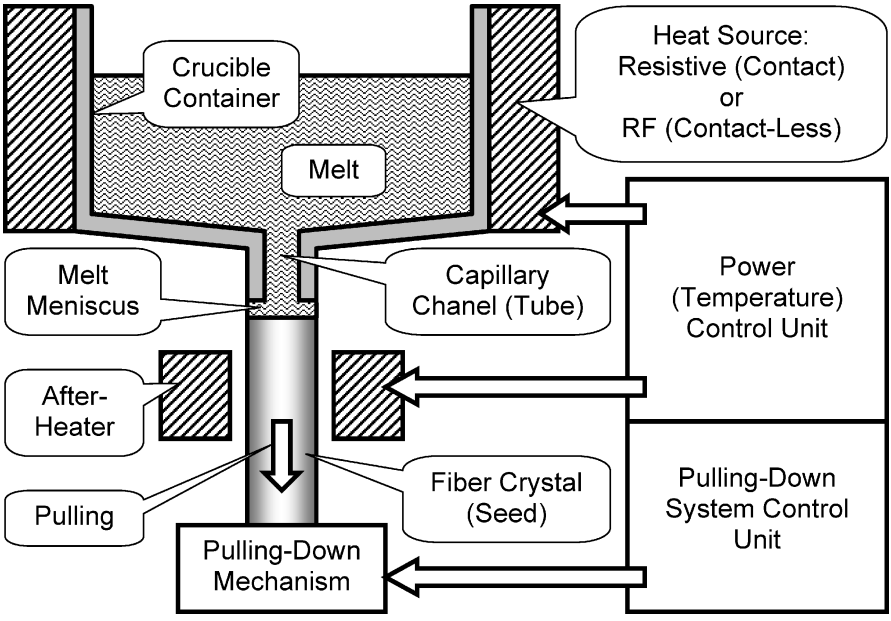

Fig. 1.2. General schematic diagram of μ-PD system

The abbreviation "μ-PD" has been widely used since 1992–93, when the first modern design of resistively heated μ-PD apparatus was created in Tohoku University, Japan, for the growth of $LiNbO_3$ [4–6] and $K_3Li_2Nb_5O_{15}$ [7,8] thin-fiber crystals. Soon after, a prototype μ-PD apparatus with a radiofrequency (RF) inductive heater was built to produce $Si_{1-x}Ge_x$ mixed (solid solution) crystals. Bulk crystal growth was achieved using graphite crucibles with multiple capillary channels [9]. However, the crucibles used to grow thin fibers had only one opening in the geometrical center of the conical bottom of the crucible container [10, 11]. Tens of other μ-PD machines have been developed and built since then. However, the general layout and the principles of the process have not changed very much. Most of μ-PD equipment reproduces the general structure of the μ-PD system illustrated in Fig. 1.2.

1.1 Internal and External Melt Heating

One of the earliest growth methods to apply pulling-down to produce $CaWO_4$ crystals similar to those shown in Fig. 1.3 (left) was reported over four decades ago [12] (see Sect. 1.3 for details). Not surprisingly, it was called the "modified floating zone recrystallization technique" by the author. Upon comparing them, the similarity of this set-up to the conventional floating zone (FZ) method quickly becomes apparent. However, one of the techniques uses a strip heater (Fig. 1.3, left), that, after appropriate development (Sect. 1.3), could play the role of the crucible, while the other technique is evidently crucibleless (Fig. 1.3, right). In spite of this fundamental difference, the schemes are

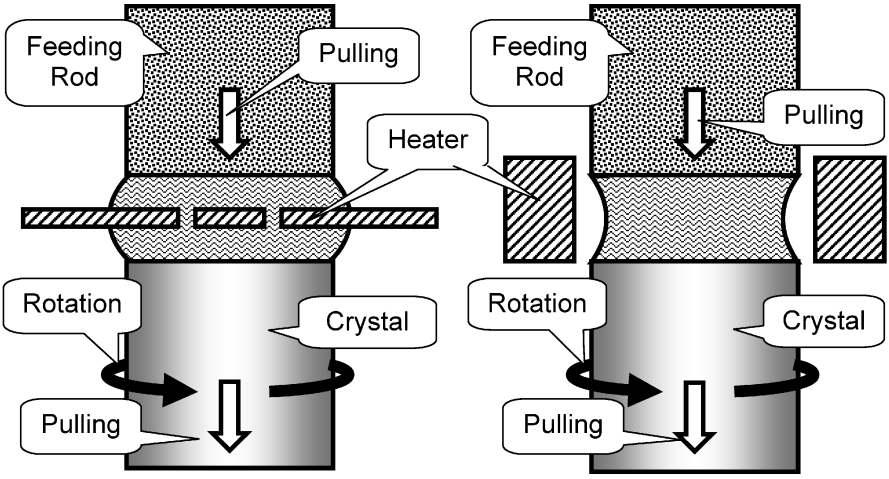

Fig. 1.3. Comparison of "modified floating zone re-crystallization technique" [12] with strip-like heater/crucible (*left*) and conventional floating zone method (*right*) corresponding to internal and external heating of the melt, respectively

almost identical except for the positioning of the heating source (internal or external with respect to the melt). The main difference between them is that the melt is not in direct contact with the heating element in one case, while it is in the other. Of course, this difference is important because it affects many significant and critical parameters that determine the final quality of the crystal, including the temperature distribution on the growth interface, the shape of the melt/crystal interface, wetting of the melt to the strip heater, and the shape of the meniscus.

In the case of internal heating, the shape of the crystal depends considerably on the shape and properties of the heater. The appearance of the heater can easily be customized, depending on the requirements, to the crystal shape and properties. Thus, the use of an internal heater provides an additional way to control the shape of the molten zone compared to the crucible-less FZ method. Needless to say, the insertion of the heater into the melt will also increase the probability of crystal contamination, which is certainly a disadvantage of an internal heater when compared to a typical crucible-less FZ (Fig. 1.3, right).

On the other hand, the direct coupling of the metal strip heater with the melt substantially decreases heat losses [13], which is another benefit of the scheme shown on the left. The quantity of molten material is also considerably smaller; the thickness of the molten zone is only 2–3 mm. Therefore, the power that needs to be supplied to the growth system can be reduced significantly, making the strip-heated system more cost-effective. In spite of the presence of a foreign substance in the melt, this method still represents a zone melting process based on two phase transitions (solid–liquid–solid or feed–melt–crystal). This makes it an attractive method for the preparation of chemically uniform crystals compared to the Czochralski (CZ) system, for example, where only one phase transition (liquid–solid) is established.

One additional advantage of internal heating is its ability to provide more accurate temperature control compared to external heating systems (optical for instance). This was particularly noted in [14], where the growth of (β_{II})-Li_3VO_4 was achieved using a "heater-in-zone" strip heater. (β_{II})-Li_3VO_4 phase formation is observed over a very narrow temperature range. Therefore, exceptionally precise temperature control was required to achieve the solidification of the single-phase material and to avoid undesired phase transformations.

1.2 Pulling Up and Pulling Down

1.2.1 Effect of Gravity

In most growth techniques, the crystals are produced through the continuous transport of the seed and the as-grown part of the crystal in the upward

direction (Fig. 1.4, left). Industrial production of high-quality crystals is generally based on such methods (CZ, typical EFG, etc.). The action of gravity in such schemes together with the directions of the temperature gradients help to separate the crystallized solid from as-yet unsolidified fluid. This simplifies the control of the growth process by separating the ordered substance (the crystal) from the predominantly chaotic one (melt). In this way, most uncontrolled events (for example vibrations or temperature fluctuations) are not accompanied by the movement of disordered melt onto the surface of the as-grown crystal followed by the fast (and uncontrolled) solidification of the liquid into polycrystalline solid. Thus, the pulling-up process is more stable than pulling-down (Fig. 1.4, right).

On the other hand, one significant advantage of pulling-down schemes is that there is a reduced probability of incorporating bubbles into the crystals, a factor that often determines the overall quality of the as grown material, especially that produced by the EFG method. The action of gravity results in the redistribution of the bubbles inside the melt such that they move to the top of the melt (Fig. 1.4, left). In the case of pulling-down growth, this movement means that most of the bubbles will be located far from the growth interface, making it unlikely that they will be "frozen" inside the crystal. This is not the case for pulling-up growth, where the crystal is positioned at the upper interface of the melt.

It is evident that the pulling direction (upward or downward) also affects the redistribution of the heavy solid particles often formed in melts due to the recrystallization of crucible material that is partially dissolved in the melt at high temperatures. The densities of Pt and Ir (the materials most often used for crucible fabrication) are 21.45 and 22.45 $\mathrm{g/cm^3}$, respectively. This is much greater than the densities of oxide crystals (and corresponding melts) such as $LiNbO_3$ (4.64 $\mathrm{g/cm^3}$), $Y_3Al_5O_{12}$ (4.57 $\mathrm{g/cm^3}$), $Bi_4Ge_3O_{12}$ (7.13 $\mathrm{g/cm^3}$).

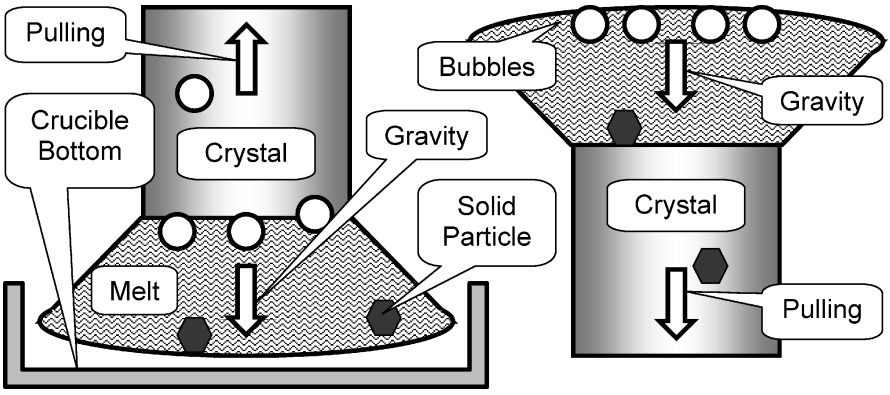

Fig. 1.4. Effect of crystal pulling direction up (*left*) and down (*right*), respectively and gravity on separation of solid from liquid and defect location (light bubbles and non-dissociated heavy solid particles)

Therefore, these particles will most likely be found in the bottom of the melt. The probability that they will be incorporated into the crystal is therefore greater when the crystals are produced using a pulling-down scheme.

1.2.2 Melt Feeding

One of the advantages of pulling-down growth is that it is relatively simple to continuously feed the melt with additional raw materials. In the case of pulling-up growth, the bottom and side interfaces of the melt are surrounded by the crucible (Fig. 1.4, left). Therefore, the only way to add extra raw material (continuous charging [15]) to the liquid in the single crucible scheme is between the crystal and the crucible wall at the top of the melt. However, this is not appropriate because the melt surface is in direct contact with the growth interface. The probability of depositing these (still solid) feed particles onto the interface and therefore the crystal is too high, potentially changing the growth of a single crystal into the solidification of a polycrystalline ingot. A higher degree of dissociation of the feed particles and a better melt homogeneity can be achieved in a double-crucible Czochralski process [16]. However, this technique requires more complicated crucible design and process control equipment and so it is often not cost-effective.

In contrast, in a pulling-down system, the top surface of the melt is generally free (Figs. 1.1–1.4) and available for feeding. The atmosphere/melt interface that absorbs the feed particles or the grains of the polycrystalline feeding rod is well isolated from the growth interface by the molten zone. This prevents immediate contact between solid particles and the crystal. Moreover, the particles have a higher porosity (and therefore a lower density) than the melt, which keeps them on the surface of the liquid for enough time for them to dissolve completely. Figure 1.4 also illustrates the general behavior of these particles if we assume that the particles behave in a similar way to bubbles due to their relatively low density.

Furthermore, the strip heater or the crucible inside the molten zone acts as an additional solid barrier, as suggested by Fig. 1.3, left. This makes the trajectory of an average particle from the atmosphere/melt interface (inlet) to the melt/crystal interface (outlet) more complicated and therefore more time-consuming. As a result, the probability that the particles completely decompose in the melt increases considerably.

1.2.3 Shaped Crystal Growth with Internal Heating

In most cases, pulling-down growth with internal heating (Fig. 1.3, left) yields shaped crystal growth because the crystallization interface is not sited on the free surface of the melt as in Czochralski or top-seeded solution growth (TSSG). The position and shape of the growth interface is determined by the position and shape of the solid heater/crucible inside the fluid. This affects the shape of the meniscus and in this way influences the shape of the

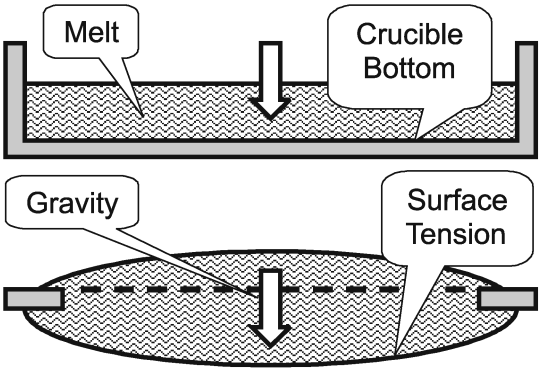

Fig. 1.5. Effect of gravity on stability of the melt for pulling-up (*above*) and pulling-down (*below*) growth

solid produced. It is generally impossible to create a free melt surface when the crystal is positioned below the melt because the melt pours out of the container in a downward direction because of gravity (Fig. 1.5).

Moreover, from practical experience of μ-PD, the inner capillary channel diameter that allows the melt to sit stationary inside the crucible reservoir (before contacting with the seed) is about 2.0 mm. This was observed in the μ-PD growth of $KNbO_3$ from a Pt crucible [17]. Similar conclusions follow from the practical application of other melt/crucible combinations. Moreover, it was demonstrated (Chap. 7, [18]) that the crystal/capillary diameter ratio can be as low as 1:6 for $Bi_4Ge_3O_{12}$ μ-PD flux growth. Taking into account both of these facts, it is expected that a μ-PD system is appropriate for pulling-down fiber growth with a negligible influence of capillary shape on crystal shape.

For pulling-up growth from the crucible, the free surface of the melt is certainly very stable due to gravity and surface tension. As a result, crystals grown via pulling-up technology from a free surface are cylindrical in shape if the anisotropy in the growth rate and subsequent faceting are not considered. Moreover, it is generally simple to create an "endless" melt surface when the crystal is positioned above the melt (Fig. 1.5, above). However, this is impossible when the crystal is growing under the melt (Fig. 1.5, below) and gravity acts as normal.

1.3 Pulling-Down Shaped Growth with Continuous Feeding

The principles of the pulling-down (PD) technique have been used for a long time, particularly for bulk crystal growth. The growth of $CaWO_4$:Nd calcium tungstate bulk crystals is one example of its use. It was first reported by

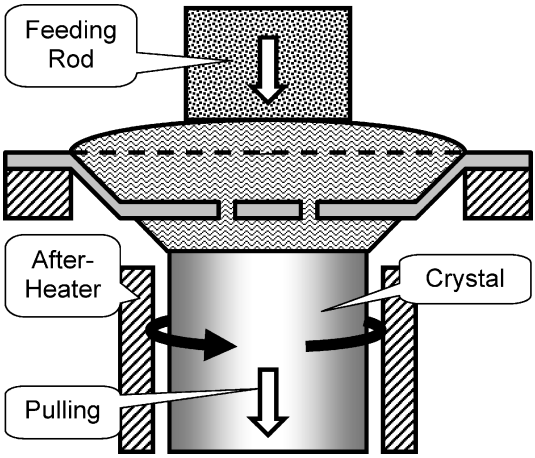

Fig. 1.6. $CaWO_4$ bulk crystal growth by "modified floating zone recrystallization technique" [12] with crystal rotation at 60 rpm

Gasson [12] in 1965 and thereafter reproduced by Takei et al. [19] in 1969 (Fig. 1.6) with an increased crystal diameter and a larger growth system. This technique did not become very popular, but it is still applied for the growth of some oxide materials [20–23]. In most cases, continuous feeding (charging) of the crucible with raw material powder is performed since it enables larger crystalline ingots to be grown, making the process industrially attractive. In this way, relatively large crystals can be produced without the need for comparatively large crucibles. Therefore, it is also considered to be a cost-effective technique.

The aspect ratios of the bulk PD crystals grown in this way are low (generally less than 10). As a result, occasional vibrations at the position of the crystallization interface have a negligible effect. This is one reason why crystal rotation is often applied during growth to improve the transport of the melt and its exchange between the neighborhood of the melt/crystal interface and volume of the melt. Note that rotation is generally not practiced when the ratio is greater than 10^2 because vibrations and the bendability of elongated crystals result in reduced shape quality (see Fig. 4.14).

1.3.1 Feeding with Polycrystalline Solid

In the $CaWO_4$ growth process reported in [12] (Fig. 1.6), a horizontal iridium strip heater ($50 \times 10 \times 1$ mm) was applied to produce the molten zone (the melting point of $CaWO_4$ is 1620 °C [12]). The crystals were rotated at 60 rpm. Two openings 1 mm in diameter were positioned symmetrically along the long axis of the strip at a distance of 6 mm. This allows the melt to pass through the heater, making transport of the feed material in the downward direction (to the growth interface) possible. When one opening in the center of the

strip positioned along the rotation axis was used, the crystals grown were found to be inhomogeneous along this axis. Cylindrically shaped crystals with dimensions of about $\varnothing\, 6 \times 50$ mm were produced using this technique at pulling-down rates of 6–12 mm/h.

A similar process was applied to the growth of YVO_4 [24] at a pulling-down rate of 5 mm/h and a rotation rate of 40 rpm. The dimensions of the iridium heating strip were $80 \times 10 \times 1$ mm (there were several holes in the middle). A charging rod of size $\varnothing\, 7 \times 100$ mm was sintered at 1400 °C for three hours. Different growth atmospheres were tested. The best molten zone stability and the largest crystal (5 mm in diameter and 18 mm long) was obtained when an argon gas flow (2 l/min) containing 0.3% oxygen was used to protect the strip heater from oxidation and to maintain the most favorable configuration of the molten zone.

Another procedure (called the "metal strip-heated zone melting technique" by the authors of [13]) was utilized recently for the growth of near-stoichiometric $LiNbO_3$. The process used was similar to that shown in Fig. 1.3, left, with coaxial rotation of both the feeding rod and the crystal. The strip heater was made of platinum and was as large as $160 \times 50 \times 1$ mm. The growth parameters used included rotation at 30 rpm and a pulling-down rate of 2 mm/h. The molten zone was 2–3 mm thick. The melt/crystal interface was comparatively flat due to the flatness of the strip heater.

It is clear that above pulling-down process is also applicable to the fabrication of polycrystalline materials, if desired. Sometimes it is impossible to grow single crystals because the chemical properties of the target material do not permit it (incongruent melting). In this case, the solidification of polycrystalline material (sometimes with portion of the second phase) with a well-developed texture can suffice. As an illustration, a process similar to that shown in Fig. 1.6 was applied to solidify highly textured $Bi_{2.1}Y_{0.1}Sr_{1.9}CaCu_{2-x}Li_xO_8$ polycrystalline ingots [25, 26] that have superconducting properties.

1.3.2 Feeding with Powder

Powder feeding is generally more appropriate from the point of view of process industrialization. The feeding rods do not need to be prepared in such a configuration, which simplifies the process. Moreover, it is not necessary to set up an upper pulling mechanism, which simplifies the apparatus; a powder supply system is used instead. An additional benefit of powder feeding is the practically unlimited ability of the growth system to produce large crystals. The length of the lower pulling mechanism is the only limitation on the amount of solidified material. It is not difficult to increase the volume of powder supplied, which means that a larger volume of crystalline material can be produced in a single growth run. Therefore, this type of apparatus is more appropriate for the mass production of crystals. A number of oxide materials, such as rutile, TiO_2 (Fig. 1.7) [20], $Bi_{12}SiO_{20}$ [21],

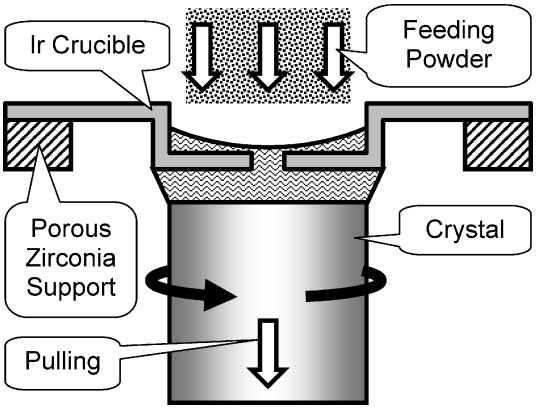

Fig. 1.7. Rutile bulk crystal growth by pulling-down technique with RF heating according to [20]

$Li_2B_4O_7$ [22], and $LiNbO_3$ [23], have been produced using powder-feeding equipment. Examples of procedures that apply this type of process are reviewed below.

Rutile (TiO_2) crystals (melting point: ∼1850 °C) were grown from a cylindrical iridium crucible 30 mm in diameter and 20 mm in height heated with RF generator. A crucible with one opening 2 mm in diameter made in the geometric center of the crucible bottom was reported [20] to be suitable for growing crystals 25 mm in diameter and up to 60 mm long. The crucible was continuously charged with TiO_2 grains in a similar fashion to that shown in Fig. 1.7. The powder contained grains of weight 0.02–0.05 g, and the powder was supplied to the crucible once every minute. The crystals were grown at a pulling-down rate of 5 mm/h with the molten zone adjusted to be 2–3 mm thick. A rotation rate of 10 rpm was applied to increase the uniformity of the melt and the overall quality of the crystal.

Attempts were also made to use sintered polycrystalline TiO_2 rods (up to $\varnothing\, 10 \times 140$ mm in size) to feed the crucible (see the previous subsection). In this case, the diameter of the crystal was controlled by optimizing the mass balance. This was achieved by choosing a suitable relationship between the pulling-down rates applied to the feeding rod and the crystal. However, the amount of recrystallized material obtained in this process (i.e., the size of the crystal grown) was limited: it was difficult to fabricate long and well-shaped cylindrical feeding rods with high aspect ratios. Attempts to increase the total amount of charged material by increasing the diameter of the feed rod resulted in the formation of very big droplets when melting. These accidents generated a step change in the total amount of the melt in the crucible and resulted in fluctuations in the crystal diameter. It is evident that the variations in the melt temperature resulting from the addition of relatively large droplets affected the stability of the process.

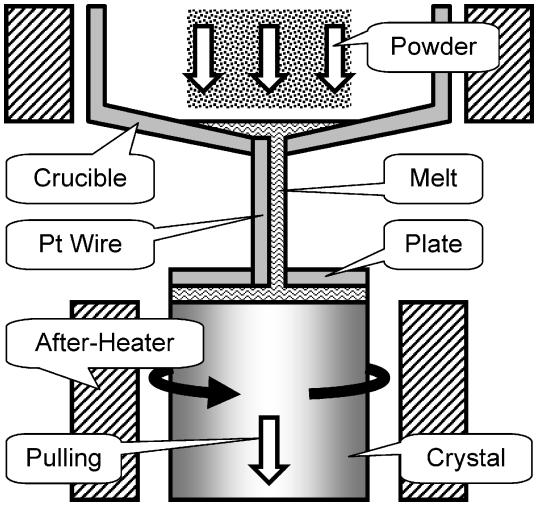

Fig. 1.8. Growth of $Bi_{12}SiO_{20}$ bulk crystals according to [21]. The heat to the crucible is supplied from external SiC resistive heater

$Bi_{12}SiO_{20}$ crystals were produced using a similar technique and rotation at 20 rpm [21]. Another innovation applied in this process was related to the (more complicated) design of the crucible. This is illustrated in Fig. 1.8. The raw material powder supplied to the crucible is first melted in the container section. It then passes through the opening in the bottom of the crucible and flows out of the crucible, guided by a Pt wire attached close to the opening at the crucible bottom. Thereafter, the melt moves into the plate shaper (the lower part of the crucible), passing through an additional opening made in the center of the plate, and finally forms a molten film between the plate and the seed during the initial stage of growth. Later on, the cross-section of the crystal is adjusted to be identical to the cross-section of the plate. The growth of bulk $Bi_{12}SiO_{20}$ crystals about 40 mm in both diameter and length has been demonstrated using this technique. The crystals were produced from the melts containing an excess of Bi_2O_3. This was necessary to compensate for Bi_2O_3 evaporation from the surface of the melt, as described in [18, 27]. The shape of the solid/liquid interface was flat, as expected from the flatness of the plate shaper (Fig. 1.8).

1.3.3 Double Strip Heater Growth

The use of the double strip heater arrangement illustrated in Fig. 1.9 was described in [28, 29]. In particular, it has been used to grow $Gd_3Sc_2Al_3O_{12}$ (melting point: 2090 °C) and other rare-earth scandium–aluminum garnet crystals [29]. However, no details (including the dimensions of the whole set-up and the quality of the crystals produced with this technique) were

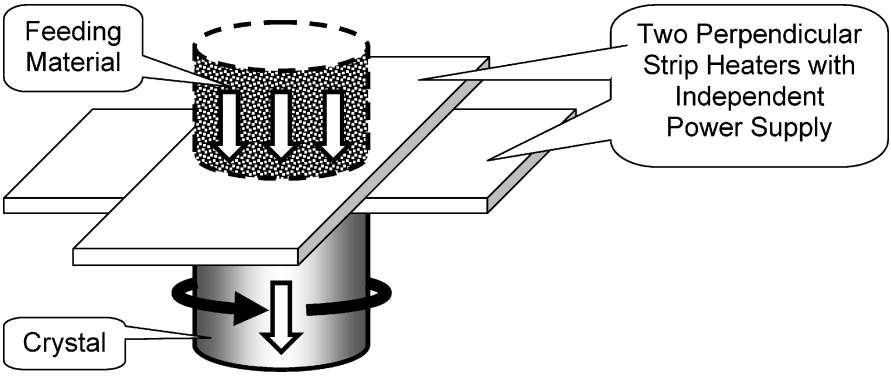

Fig. 1.9. Growth of $Gd_3Sc_2Al_3O_{12}$ garnet crystals with two perpendicular stripe heaters according to [28, 29]

reported, although the ability of the system to heat the strips independently was mentioned. This allowed independent control of position of the melting (i.e., of the feeding material) and the solidification (i.e., the as-grown crystal) interfaces. The heaters mere made of molybdenum 0.3 mm in thickness, and were 12–16 mm wide. Iridium heaters were also applied and these were $80 \times 16 \times 0.3$ mm in size.

A number of additional shapers allowing the growth of bulk cylindrical crystals as well as plates, tubes, and other shaped ingots were also designed and introduced in [28, 29]. The top sections of these schemes were generally similar to those shown in Figs. 1.6 and 1.7, with either polycrystalline rod or powder feeding. However, the lower sections of the crucibles (the heaters) had more complicated profiles corresponding to the desired shape of the solidified material. Unfortunately, practical applications of these schemes to the growth of actual crystals were not mentioned.

1.3.4 Flux Growth with Traveling Solvent

It is evident (especially from Fig. 1.3, left) that μ-PD growth with traveling solvent, similar to that practiced by means of a more conventional FZ set-up (Fig. 1.3, right), is also possible when feeding material is constantly supplied to the melt in the solid state (as a polycrystalline rod or a powder of constant chemical composition). This is a significant advantage of continuously feeding system because it allows a constant melt composition to be maintained throughout the entire growth process except for the initial and final stages. This is especially important for crystals that melt incongruently and for growth conditions that require that the compositions of the original liquid (the melt) and the resulting solid (the crystal) are somewhat different. A similar environment is desirable for the growth of doped crystals when the segregation coefficient of the dopant dif-

fers greatly from unity. Application of a traveling solvent allows the production of crystals with fundamentally uniform distributions of all constituents along the growth axis when the composition of the feed solid is constant.

An example of such a process was reported in [14] for the growth of (β_{II})-Li_3VO_4 single crystals (a nonlinear optical material used for second harmonic generation) with $LiVO_3$ flux. The platinum strip heater used contained many openings, each of which were 0.8 mm in diameter, and the temperature of the heater was controlled via a thermocouple. The growth rates applied in this flux growth process were 0.25–1.00 mm/h, which were somewhat lower than those applied for melt growth [12, 13, 24] when the compositions of the melt and the crystal were equal. Low growth rates are required for any flux growth independent of the design of the system used because redistributing and reordering the particles transported from liquid mass to the growth interface takes time (see Chap. 4). The rotation rate of the crystal varied from 10 to 30 rpm. However, no rotation was applied to the feeding rod. The crystals were 20–30 mm long with diameters of about 3 mm. The crystals grown with a low pulling-down rate of 0.25 mm/h and a fast rotation rate of 30 rpm were bubble-free. The effects of both the pulling rate and the rotation rate on bubble formation in the solid can be gauged from Fig. 1.4, right. Moreover, a positive influence of melt stirring on the elimination of gas-containing defects was also noticed in [30].

The scheme used for (β_{II})-Li_3VO_4 flux growth was generally identical to that shown in Fig. 1.3, left. The molten zone contained a flux surplus, making it possible to form the target phase. The compositions of the incoming and outgoiing solids were generally equal, as normally anticipated for the conventional traveling solvent (flux) technique; both were automatically balanced due to the presence of the extrastoichiometric flux in the intermediate fluid between the two solids.

Growth with a traveling solvent cannot be realized in a feedless process like conventional Czochralski or EFG. However, all of the above schemes (Figs. 1.3, left, 1.6–1.9) that involve feeding can be used for this technique. Both of the schemes in Fig. 1.3 become practically identical when the principles of traveling solvent use (intentional mismatch of the compositions of the feed rod and the melt) are applied to growth from flux.

1.4 Pulling-Down Shaped Growth without Feeding

1.4.1 Solid/Liquid Interfaces and Melt Homogeneity

One of the most important disadvantages of the schemes with feeding presented in previous section (Figs. 1.6–1.9) follows from the existence of the additional solid/liquid interface in the growth system [31], as shown in Fig. 1.10.

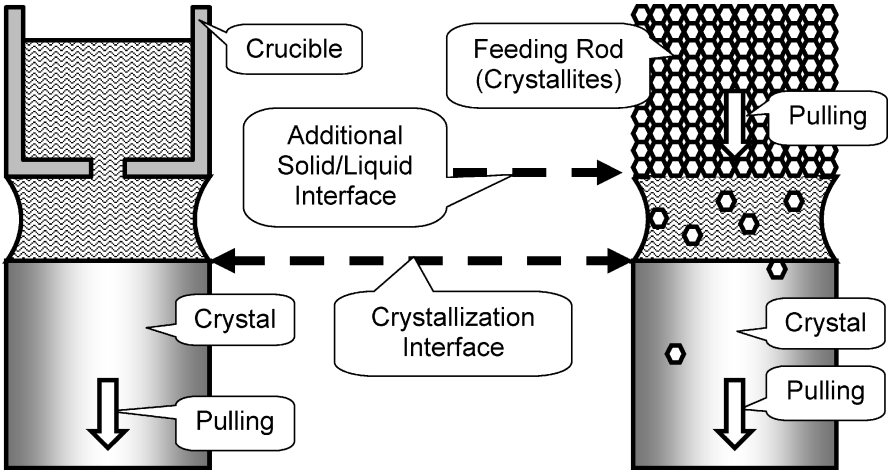

Fig. 1.10. Illustration of effect of additional solid/liquid interface on crystal quality according to [31]

Solid particles (crystallites or grains) of feed substance in those systems are continuously introduced into the melt. A significant period of time is generally needed for these particles to completely dissociate. The time required depends on the intensity of mass exchange that occurs inside the fluid (due to free and forced convection, thermocapillary flows and diffusion), the height of the molten zone, and the temperature. It is also a function of the strength of the chemical bonds in the starting solid, which determines the rate of dissolution of the crystallites in the melt. Thus, the probability that the crystallites in the melt have not dissolved completely in the melt before coming to contact with the growth interface is generally greater than zero. This means that these particles can also bond to the crystal during pulling-down. This transforms single-crystal growth into the solidification of polycrystalline material. Note that this phenomenon has little to do with density effects (Fig. 1.4, right) because the densities of a liquid and a solid of same composition are practically equal.

As a result, the structural quality of crystals grown in systems with two solid/liquid interfaces (Fig. 1.10, right) is generally lower than those produced from a single-phase homogeneous melt situated in the crucible (Fig. 1.10, left). If we consider fiber crystal growth, the schemes shown in Fig. 1.10 correspond well to the μ-PD and LHPG (or FZ) techniques, respectively (left and right). The growth of single-crystalline materials from homogeneous melts (with one liquid/solid interface and without feeding) is discussed in detail below. In general, the chemical homogeneity and the structural uniformity of such a fluid (Fig.1.10, left) are ensured by considerable overheating and/or by maintaining the melt at a constant temperature well above the melting point.

1.4.2 Micro-Pulling-Down Growth

The typical micro-pulling-down system shown in Fig. 1.2 yields the growth of thin fiber crystals (with high aspect ratios) without feeding and with one solid/liquid interface. A number of other examples (crucible designs, procedures, etc.) of crystal growth based on this scheme are considered in detail in Chaps. 5–23. Crucibles with conical bottoms are normally used to grow fiber type crystals about 1 mm in diameter. However, those applied for the growth of bulk and/or shaped crystals generally have more complicated profiles at the bottom (i.e., a die).

For some highly wettable melts, bulk crystals can also be produced with dimensions that are close to the external diameter of the crucible. This was demonstrated in particular for the growth of $Tb_3Ga_5O_{12}$ garnet crystals [32], as shown in Fig. 1.11. Crystals with diameters of up to 10 mm were grown from an ordinary μ-PD crucible initially designed for the growth of fiber materials (note the conical shape of the bottom of the crucible).

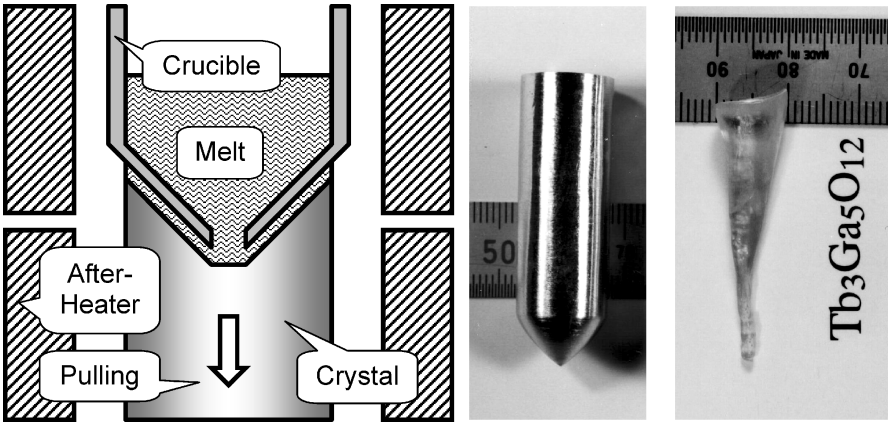

Fig. 1.11. Growth of bulk $Tb_3Ga_5O_{12}$ garnet crystal according to [32]: diagram (*left*), crucible (*center*), and as grown crystal (*right*)

1.5 Pulling-Up Shaped Growth without Feeding

Pulling-up is the most popular direction of growth. It is applied in numerous growth techniques, including the Czochralski method (see Sect. 1.2 for details). However, all solidification processes that are performed from the free surface of the melt are not discussed here; specifically we overlook the cases where the shape of the crystal is controlled exclusively by surface action (tension) and the anisotropy in the growth rate (crystallographic structure of the solid). However, we do discuss processes where the shape of the crystal is

determined by surface action between two solid materials (a crucible/shaper that does not interact with the melt, and the crystal that is produced from the melt). Thus, we can classify most of the pulling-up melt growth techniques known into the following three types:

(1) Those with the melt between the crystal and a chemically inert crucible die (EFG)
(2) Those with the melt between the crystal and the solid feeding material (FZ and LHPG)
(3) Those with just an "endless" melt and the crystal (Czochralski; see Fig. 1.4, left).

In this section, usually only those of type (1) using the upward pulling direction are discussed since they have the most features in common with the pulling-down process illustrated in Figs. 1.2, 1.6–1.8, and 1.11. The effect of changing the system such that gravity acts opposite to the direction of crystal growth, a situation encountered when the melt is placed between the die material and the crystal, is now overviewed.

1.5.1 Edge-Defined Film-Fed Growth (EFG/Stepanov)

In terms of the geometry of the experimental set-up, the growth of a shaped crystal by the edge-defined film-fed (EFG) or Stepanov technique [30, 33–35] is the method most similar to the μ-PD process. In most cases it is performed such that displacement of the as-produced solid occurs continuously in the upward direction. The process itself is based on the continuous conversion of shaped fluid into solid. The formation of a shaped fluid (or a liquid column) is achieved through the application of a solid shaper element that provides

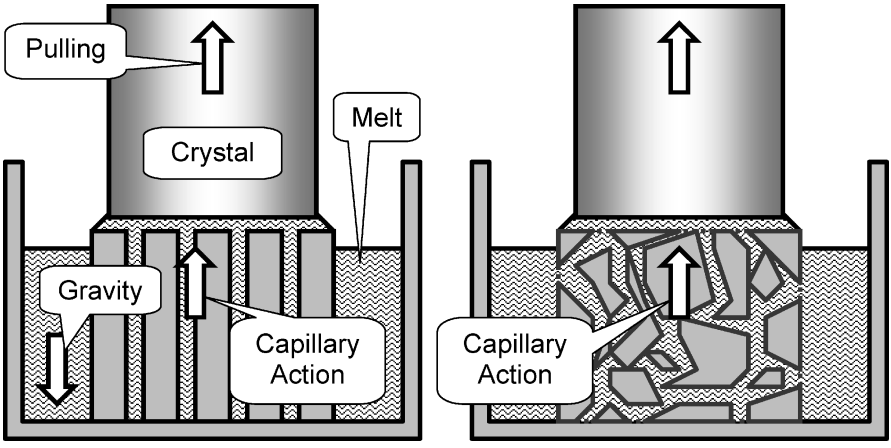

Fig. 1.12. Schematic diagram of EFG technique (*left*) and variation of that with porous iridium ingot according to [36]

the liquid/solid interface with the melt through the column (Fig. 1.12). The shape of the column is determined by the configuration of the shaper or die.

In the case of the conventional pulling-up EFG process, a fluid film is formed on the top of the shaper element containing one or a number of capillary channels, as shown in Fig. 1.12, left. These channels makes it possible for the melt to rise to the top of the die through the action of capillary forces. It should be noted here that in this arrangement gravity acts in the direction opposite to crystal growth, unlike the situation in the μ-PD process (Fig. 1.2). Nevertheless, movement of the melt in the upward direction is generally achievable, depending on the wetting properties of the fluid.

The shapes of the channels can also be more complicated than this, as shown in Fig. 1.12, right. Therefore, the application of porous shapers that contain a natural capillary network is also possible [36]. Consider the porous die shown in Fig. 1.13. Relatively few studies of the application of porous materials to shaped crystal growth have been published so far, but the idea appears to be very promising, especially considering its potential to suppress the segregation that is easily detectable in number of μ-PD processes [18, 31, 37–39].

EFG growth is often considered to be an attractive industrial technique because a shape different to a cylinder (as obtained with CZ-grown crystals) is necessary for most applications related to actual devices. It is assumed

Fig. 1.13. Porous Ir die ($\varnothing$ 27 mm) used in pulling-up EFG process. *Left view* represents actual position of the die in the growth (Fig. 1.12, *right*). The die was used for the growth of rare-earth vanadate crystals with details available in [36] (Courtesy of V.V. Kochurikhin, 2005)

that the production of shaped crystals (mostly slices or plates) eliminates the large losses of single crystalline material enduring when a cylindrical bulk crystal is cut. However, EFG crystals often have low levels of crystallographic perfection (compared with those produced by CZ method), and this is often seen as an unavoidable disadvantage of EFG technology [40].

1.5.2 Effect of Die Properties on Melt Behavior

One important requirement for successful EFG growth procedure is to keep the melt level in the crucible high enough to maintain complete contact between the melt and the crystal (indeed, this is a vital requirement for any crystal growth technique). Therefore a measurement of the capillary action is commonly needed before the shape of the die and its capillaries can be designed, and before the process can be configured. This can be achieved using a capillary-forming guide made from a couple of plates of the material that is intended for use as the shaper material. An example of this type of guide, produced from iridium plates welded together [41], is illustrated in Fig. 1.14. A guide with a maximum slot thickness of 5 mm was applied to study the behavior of melts of TiO_2 [41] and the rare-earth vanadates YVO_4 and $GdVO_4$ [31].

The dependence of the capillary height (h) on the slot width (t) is reported [41, 42] to be well described by following equation:

$$h = \frac{2\gamma \cos\theta}{\rho t g} \,, \tag{1.1}$$

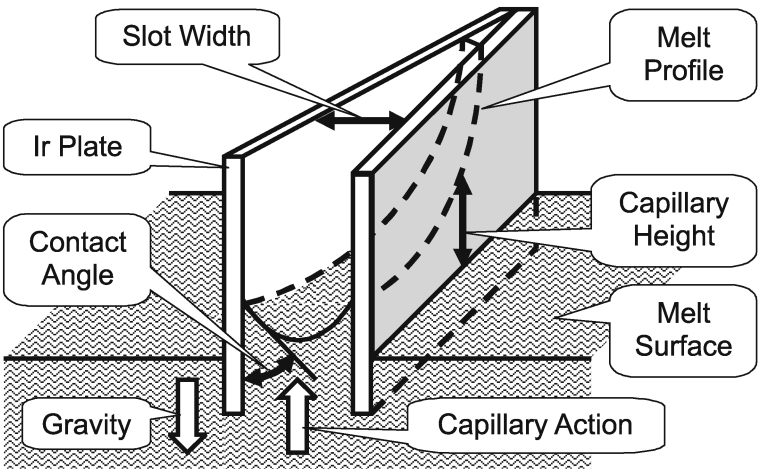

Fig. 1.14. Schematic diagram of measurement of capillary action with capillary-forming guide according to [41]

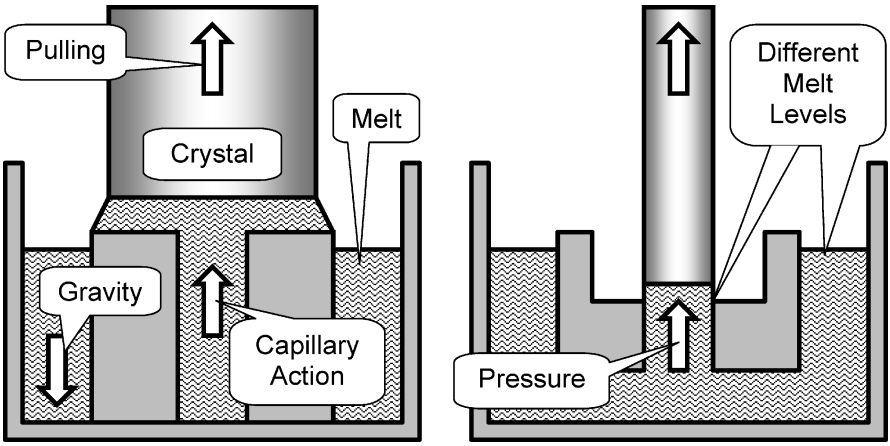

Fig. 1.15. Effect of wetting properties of performance of the melt column in shaped crystal growth

where γ is the surface tension, θ is the contact angle, ρ is the density of the melt, and g is the gravitational acceleration.

EFG growth according to the schemes shown in Fig. 1.12 generally requires good wetting between the die and the melt (Fig. 1.15, left). In the opposite case, additional pressure should be applied outside of the die to promote upward melt flow from the body of the melt to the liquid film that is in contact with the edges of the shaper. This can also be done by displacing the shaping element in the downward direction. As a result, the hydrostatic pressure that is originated from the difference in the melt levels inside and outside of the shaper allows melt to be supplied to the growth interface. This case is demonstrated in Fig. 1.15, right.

As for the pulling-down EFG configuration, the effect of wetting properties on the ability of the system to support contact between liquid and solid is not as critical as in the case of the pulling-up system shown in Fig. 1.2. In the pulling-down set-up, the action of gravity aids the flow of the melt in the downward direction, even when the hydrostatic pressure is relatively low (for melt levels of just a few millimeters). Therefore, a number of melts that are nonwettable with respect to the crucible material have been successfully used for actual μ-PD crystal growth. $Y_3Al_5O_{12}$ garnet fiber crystal growth [31] is one such process.

1.5.3 Inverted EFG/Stepanov Growth

If we think about the geometry of the growth system used, the μ-PD technique can be considered to be a particular variant of the so-called inverted EFG/Stepanov technique [30]. Almost all of the characteristics and properties that are representative of the EFG/Stepanov set-up can also be found

in the μ-PD system. In both schemes, the shape of the crucible determines the shape of the crystal grown. Moreover, the crystal is produced from the liquid film that is situated between the die and the solidified material, and the solid is pulled in the downward direction.

However, the melt performance (melt exchange, segregation, etc.) of a conventional μ-PD system (see Fig. 1.2) is often different from that of the EFG technique. In some cases it is comparable to the Czochralski scheme due to miniaturization and strong Marangoni convection [39]. A detailed comparison of these techniques is presented in Chaps. 5 and 6.

1.6 History and Popularity of μ-PD

While it is not the purpose of this chapter to provide a complete history of the development of μ-PD crystal growth techniques, in terms of both the development of the equipment used and the materials produced with this method, it is interesting to list some important facts, events and innovations that have resulted in the present status of this technology. Table 1.1 lists

Table 1.1. Selected events and/or innovations resulting in the development of μ-PD apparatus and methodology from 1993 to the present

Year	Event/Innovation	Heating	Crystal	Reference
1993	Fiber growth	RES	$LiNbO_3$	[5–8]
1995	Graphite crucible, multichannel	RF	Si–Ge bulk	[9]
1996	Graphite crucible	RF	Si–Ge fiber	[10]
1996	Melt optimization by μ-PD	RES	$Ca_3(Li,Nb,Ga)_5O_{12}$	[43]
1997	Concentric die-in-die crucible	RES	Mn:$LiNbO_3$	[44]
1998	Ir crucible and afterheater	RF	eutectic	[45]
1998	Oxide crystal, Ir crucible	RF	$Y_3Al_5O_{12}$	[31]
1998	Flux crystal growth	RES	$KNbO_3$	[17, 37]
1998	In situ orientation correction	RES	$KNbO_3$	[17, 37]
1999	$\varnothing$ 10 mm bulk crystal growth	RF	$Tb_3Ga_5O_{12}$	[32]
2000	Textured polycrystalline fiber	RES	$Bi_2Sr_2CaCuO_y$	[46]
2003	Fluoride fiber growth	RF/RES	PrF_3, LiF	[47, 48]
2003	Application of growth chamber	RF/RES	PrF_3, LiF	[47, 48]
2005	Application of Re crucible	RF	Y_2O_3	[49]
2005	Crystal weight measurement	RF	$Y_3Al_5O_{12}$	[50]
2005	1-m-long fiber crystal	RF	$Y_3Al_5O_{12}$	[50]
2006	Diameter control by evaporation	RES	$Bi_4Ge_3O_{12}$	[18]
2006	$\varnothing$ 50 µm, stationary growth	RES	$Bi_4Ge_3O_{12}$	[18]
2006	Shaped (non-cylinder) growth	RF	Sapphire	Chap. 16
2006	Multicrystal growth	RF	Pr:$Lu_3Al_5O_{12}$	Chap. 3
2006	Continuous feeding	RF	Pr:$Lu_3Al_5O_{12}$	Chap. 3

some of the events that are relevant to the development of this method and which are discussed in current and following chapters.

It would not be accurate to consider every type of μ-PD system to be a particular variant of the inverted EFG technique [39]. Therefore the term "micro-pulling-down" has become very popular over the past decades. Even a quick search through Internet databases that accumulate information on the number of citations of particular phrases clearly demonstrates that the term "μ-PD" is widely used in both scientific literature (journals) as well as in other sources of information (webpages, reports, in advertising). This is illustrated by Table 1.2, where this information is listed along with other

Table 1.2. Number of references to various phrases retrieved by various Internet search engines and scientific databases (the terms "crystal" and "growth" were also included in each search) as of December 12, 2006 [51–54] (data obtained from Science Direct using the "full text" option are from 1994 onwards)

"Phrase" + crystal + growth	Google	Yahoo	Scirus Total	Scirus Journal	Science Direct
"Liquid phase epitaxy"	89 000	2300	7018	2994	757
"Czochralski method"	80 900	1740	5634	2622	1370
"Floating zone method"	28 300	487	1755	968	462
"Edge defined film"	14 400	597	936	335	107
"Laser-heated pedestal"	12 000	330	658	343	160
"TSSG"	10 400	233	638	411	342
"Micro-pulling-down"	707	171	4590	440	127
"Kyropoulos method"	677	200	161	127	30
"Verneuil method"	435	82	240	140	27
"Stepanov method"	298	95	121	82	27

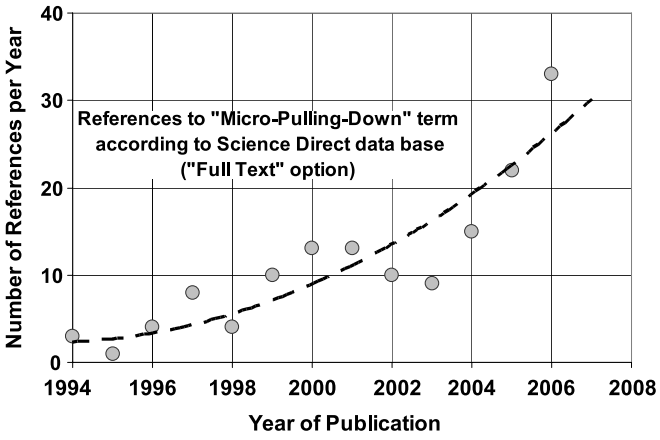

Fig. 1.16. Number of references on "Micro-pulling-down" phrase per year according to Science Direct data base [54]

terms and phrases that represent related crystal growth methods commonly used within the crystal growth community. Surprisingly, the total number of references to μ-PD in these sources was sometimes more frequent than references to classical growth techniques such as Kyropulos, Verneuil, and Stepanov. This is another reason why the term "micro-pulling-down" was used in the title of this book.

The trend line presented in Fig. 1.16 provides a visual illustration of the popularity of the μ-PD crystal growth method in terms of the number of times the method is referred to in publications from a particular year. Note that the term "micro-pulling-down" dates back to 1993–1994, when the general principles of this system were published for the first time, and so the plot only reaches back that far. Also, the Fig. 1.16 represents the reports found in just one particular data base [54], which does not cover all of the institutions involved in publishing research reports on crystal growth, and so the plot is included here for illustrative purposes only. However, a general increase in the popularity of μ-PD is evident from the plot.

1.7 Summary

Practically all of the schemes described in this chapter will seem to be relatively simple to those who are familiar with crystal growth. Using appropriate heating elements and temperature gradients and accurately controlling the power supplied to the heater, and therefore the shape and length of the molten zone, permits controllable solidification of the fluid and therefore a level of control over crystal quality. These are the principles behind any crystal growth process. However, any attempt to reproduce any of these crystal growth set-ups practically will require exceptional skills and experience from the experimentalist; it is generally not an easy task.

It is also difficult to monitor the process visually during operation. High temperatures and chemical interactions of the constituents of the melt with the ceramic insulators, supports and especially window materials make it difficult for the operator to observe the actual behavior of the system. The situation is even worse when a chemically aggressive environment (as in case of fluoride crystal growth) is necessary. Weight measurement through the application of loading cells, a practice widely used with the Czochralski method, provides a way to automate process control, but the physical ability of the weighing system to measure the weight of the crystal accurately enough is often not sufficient.

The μ-PD technique is relatively young compared to other related methods overviewed in this chapter. However, it is growing rapidly in popularity, as illustrated by Table 1.2 and Fig. 1.16.

References

1. T. Fukuda, P. Rudolph, S. Uda, (eds.), *Fiber Crystal Growth from the Melt* (Springer, Berlin, 2004)
2. P. Rudolph, T. Fukuda, Cryst. Res. Technol, **34,** 3 (1999)
3. D.H. Yoon, Opto-Electron. Rev., **12**(2), 199 (2004)
4. D.H. Yoon, I. Yonenaga, T. Fukuda, N. Ohnishi, J. Cryst. Growth, **142**, 339 (1994)
5. D.H. Yoon, T. Fukuda, J. Cryst. Growth, **144**, 201 (1994)
6. D.H. Yoon, I. Yonenaga, T. Fukuda, Crys. Res. Technol, **29**(8), 1119 (1994)
7. D.H. Yoon, M. Hashimoto T. Fukuda, Jpn. J. Appl. Phys., **33**, 3510 (1994)
8. D.H. Yoon, P. Rudolph, T. Fukuda, J. Cryst. Growth, **144**, 207 (1994)
9. H.J. Koh, T. Fukuda, Crys. Res. Technol, **31**(2), 151 (1996)
10. N. Schäfer, T. Yamada, K. Shimamura, H.J. Koh, T. Fukuda, J. Cryst. Growth, **166**, 675 (1996)
11. H.J. Koh, N. Schäfer, K. Shimamura, T. Fukuda, J. Cryst. Growth, **167**, 38 (1996)
12. D.B. Gasson, J. Sci. Instrum., **42**, 114 (1965)
13. D.Q. Ni, W.Y. Wang, D.F. Zhang, X. Wu, X.L. Chen, K.Q. Lu, J. Cryst. Growth, **263**(1–4), 421 (2004)
14. M. Higuchi, Y. Chuman, T. Kitagawa, K. Kodaira, J. Cryst. Growth, **216**, 322 (2000)
15. S.J. Kan, M. Sakamoto, Y. Okano, K. Hoshikawa, T. Fukuda, J. Cryst. Growth, **119**, 215 (1992)
16. S.J. Kan, M. Sakamoto, Y. Okano, K. Hoshikawa, T. Fukuda, J. Cryst. Growth, **128**, 915 (1993)
17. V.I. Chani, K. Nagata, T. Fukuda, Ferroelectrics, **218**, 9 (1998)
18. V.I. Chani, K. Lebbou, B. Hautefeuille, O. Tillement, J.-M. Fourmigue, Cryst. Res. Technol., **41**(10), 972 (2006)
19. F. Takei, S. Takasu, J. Ushizawa, M. Sakurai, Optoelectric Mater., **24**(12), 1507 (1969) (in Japanese)
20. M. Higuchi, T. Togi, K. Kodaira, J. Cryst. Growth, **203**(3), 450 (1999)
21. S. Maida, M. Higuchi, K. Kodaira, J. Cryst. Growth, **205**(3), 317 (1999)
22. K. Suzuki, M. Higuchi, K. Kodaira, in *The 1st Asian Conference on Crystal Growth and Crystal Technology*, Tohoku University, Sendai, Japan, 29 August – 1 September, 2000, W-P-57
23. K. Kodaira, T. Kitagawa, Y. Miyamoto, M. Higuchi, in *The 1st Asian Conference on Crystal Growth and Crystal Technology*, Tohoku University, Sendai, Japan, 29 August – 1 September, 2000, W-P-105
24. K. Muto, K. Avazu, Jpn. J. Appl. Phys., **8**, 1360 (1969)
25. P. Prabhakaran, A. Thamizhavel, R. Jayavel, C. Subramanian, J. Cryst. Growth, **183**, 573 (1998)
26. P. Prabhakaran, C. Subramanian, Supercond. Sci. Technol., **11**, 788 (1998)
27. J.B. Shim, J.H. Lee, A. Yoshikawa, M. Nikl, D.H. Yoon, T. Fukuda, J. Cryst. Growth, **243**, 157 (2002)
28. A.A. Mayer, *Protsessi Rosta Kristallov* (Processes of Crystal Growth). (RHTU im. D.I. Mendeleeva, Moscow, 1999) (in Russian)
29. I.A. Scherbakov (ed.), *Trudi Instituta Obschej Fiziki* (Proceedings of General Physics Institute), Vol. 26 (Nauka, Moscow, 1990), p. 95 (in Russian)

30. P.I. Antonov, V.N. Kurlov, Prog. Cryst. Growth Ch., **44**, 63 (2002)
31. V.I. Chani, A. Yoshikawa, Y. Kuwano, K. Hasegawa, T.Fukuda, J. Cryst. Growth, **204**, 155 (1999)
32. V.I. Chani, A. Yoshikawa, H. Machida, T. Satoh, T. Fukuda, J. Cryst. Growth, **210**(4), 663 (2000)
33. A.V. Stepanov, *The Future of Metalworking* (Lenizdat, Leningrad, 1963) (in Russian)
34. H.E. LaBelle Jr., A.I. Mlavsky, Nature, **216**, 574 (1967)
35. V.N. Kurlov, in *Encyclopedia of Materials: Science and Technology*, ed. by K. H. J. Buschow et al. (Elsevier, Amsterdam, 2001), p. 8259
36. V.V. Kochurikhin, A.V. Klassen, E.V. Kvyat, M.A. Ivanov, J. Cryst. Growth, **296**, 248 (2006)
37. V.I. Chani, K. Shimamura, T. Fukuda, Cryst. Res. Technol. **34**, 519 (1999)
38. S. Ganschow, D. Klimm, B.M. Epelbaum, A.Yoshikawa, J. Doerschel, T. Fukuda, J. Cryst. Growth, **225**, 454 (2001)
39. B.M. Epelbaum, G. Schierning, A. Winnacker, J. Cryst. Growth, **275**, e867 (2005)
40. J.C. Brice, Rep. Prog. Phys., **40**, 567 (1977)
41. H. Machida, K. Hoshikawa, T. Fukuda, Jpn. J. Appl. Phys., **31**(7B), L974 (1992)
42. B.M. Epelbaum, K. Shimamura, K. Inaba, S. Uda, V.V. Kochurikhin, H. Machida, Y. Terada, T. Fukuda, Cryst. Res. Technol., **34**(3), 301 (1999)
43. Y.M. Yu, V.I. Chani, K. Shimamura, T. Fukuda, J. Cryst. Growth, **171**, 463 (1997)
44. B.M. Epelbaum, K. Inaba, S. Uda, K. Shimamura, M. Imaeda, V.V. Kochurikhin, T. Fukuda, J. Cryst. Growth, **179**, 559 (1997)
45. A. Yoshikawa, B.M. Epelbaum, T. Fukuda, K. Suzuki, Y. Waku, Jpn. J. Appl. Phys., **38**(1A/B), L55 (1999)
46. K. Lebbou, A. Yoshikawa, M. Kikuchi, T. Fukuda, M.Th. Cohen-Adad, G. Boulon, Physica C, **336**, 254 (2000)
47. A. Yoshikawa, T. Satonaga, K. Kamada, H. Sato, M. Nikl, N. Solovieva, T. Fukuda, J. Cryst. Growth, **270**(3/4), 427 (2004)
48. M.E. Santo, B.M. Epelbaum, S.P. Morato, N.D. Vieira, Jr., S.L. Baldochi, J. Cryst. Growth, **270**(1/2), 121 (2004)
49. J.H. Mun, A. Novoselov, A Yoshikawa, G. Bpulon, T. Fukuda, Mater. Res. Bull., 40, 1235 (2005)
50. K. Lebbou, D. Perrodin, V.I. Chani, O. Aloui, A. Brenier, J.M. Fourmigue, O. Tillement, J. Didierjean, F. Balembois, P. Gorges, J. Am. Ceram. Soc., **89**(1), 75 (2006)
51. Google Inc., *Google Search Engine*, Accessed February 12, 2007, http://www.google.com/
52. Yahoo! Inc., *Yahoo Search Engine*, Accessed February 12, 2007, http://www.yahoo.com/
53. Elsevier B.V., *Scirus Search Engine*, Accessed February 12, 2007, http://www.scirus.com/srsapp/
54. Elsevier B.V., *ScienceDirect Website*, Accessed February 12, 2007, http://www.sciencedirect.com/

http://www.springer.com/978-3-540-71294-7

Shaped Crystals
Growth by Micro-Pulling-Down Technique
Fukuda, T.; Chani, V.I. (Eds.)
2007, XV, 341 p., Hardcover
ISBN: 978-3-540-71294-7